Journal of Solid State Chemistry **142,** 146–151 (1999)
Article ID jssc.1998.8003, available online at http://www.idealibrary.com on IDEAL®

Electrical and Magnetic Properties of $La_{1-x}Ce_xRu_4P_{12}$ and $CeOs_4P_{12}$ with the Skutterudite Structure

Ichimin Shirotani, Takanori Uchiumi, Chihiro Sekine, Masahisa Hori, and Shigeyuki Kimura

Muroran Institute of Technology, 27-1, Mizumoto, Muroran-shi 050-8585, Japan

and

Nozomu Hamaya

Faculty of Science, Ochanomizu University, Bunkyo-ku, Tokyo 112, Japan

Received October 7, 1997; in revised form August 12, 1998; accepted August 13, 1998

The crystal structures of $LaRu_4P_{12}$ and $CeRu_4P_{12}$ are refined by the Rietveld analysis of the powder *X*-ray diffraction data. The bond distances and bond angles in both phosphides are obtained. $La_{1-x}Ce_xRu_4P_{12}$($x = 0$, 0.1, 0.2, 0.3, 0.4, 0.5, 0.6, 0.7, 0.75, 0.8, 0.9, and 1) and $CeOs_4P_{12}$ are prepared at high temperatures and high pressures. Powder X-ray diffractions of the alloys are studied at room temperature. The lattice parameters of the alloys do not change linearly with increasing x and markedly deviate from linear between $x < 0.4$ and $x = 0.6$. The formal oxidation number of Ce atoms in the alloys is +3 below $x = 0.6$. The electrical and magnetic properties of the alloys $CeRu_4P_{12}$ and $CeOs_4P_{12}$ are studied at low temperatures. The metal-to-insulator transition and magnetic ordering appear at around $x = 0.6$. Above $x = 0.7$ the alloys behave as a semiconductor. $CeOs_4P_{12}$ exhibits a semiconducting behavior, with an activation energy of 0.034 eV. $CeRu_4P_{12}$ and $CeOs_4P_{12}$ show a very small, nearly temperature-independent susceptibility. Electrical and magnetic properties of the alloys, $CeRu_4P_{12}$ and $CeOs_4P_{12}$ are discussed.

INTRODUCTION

Ternary metal phosphides with the general formula LnT_4P_{12} (T = Fe, Ru, and Os; Ln = lanthanide) crystallize with a skutterudite structure filled by lanthanide atoms (1, 2). The Ln atoms are located at (000) and (1/2, 1/2, 1/2) in the cubic structure. The transition-metal atoms are in the center of a distorted octahedron of six phosphorus atoms. The skutterudite structure is characterized by formation of well-defined P_4 groups.

$CeFe_4P_{12}$ and $CeRu_4P_{12}$ show semiconducting behavior over the range 2–300 K (3,4). These phosphides have a smaller lattice parameter than that expected for the trivalent Ce ion. The reduced cell volumes of CeT_4P_{12} (T = Fe, Ru, and Os) suggest the formal oxidation number +4 for the Ce atoms (1). When all bonding electrons are counted as belonging to phosphorus atoms, the Ru atoms in $CeRu_4P_{12}$ have a d^6 configuration. Jung *et al.* suggest according to the band calculation that the skutterudite compounds are expected to be semiconducting if their transition-metal electron configuration is d^6 but metallic in other cases (5). On the other hand, Nordstrom and Singh point out that Ce atoms in $CeFe_4P_{12}$ are trivalent and Ce 4*f* states hybridize strongly with Fe 3*d* and phosphorus *p* states in the vicinity of the Fermi energy; the gap formation in $CeFe_4P_{12}$ is due to these hybridizations (6).

We have prepared $La_{1-x}Ce_xRu_4P_{12}$ (x = 0, 0.1, 0.2, 0.3, 0.4, 0.5, 0.6, 0.7, 0.75, 0.8, 0.9, and 1) and $CeOs_4P_{12}$ with the skutterudite structure at high temperatures and high pressures (7). The electrical and magnetic properties of the alloys $CeRu_4P_{12}$ and $CeOs_4P_{12}$ have been studied at low temperatures. The position of phosphorus atoms in $LaRu_4P_{12}$ and $CeRu_4P_{12}$ is determined with the Rietveld method of analyzing powder X-ray diffraction data. In this paper the electrical and magnetic properties of the alloys $CeRu_4P_{12}$ and $CeOs_4P_{12}$ are discussed.

EXPERIMENTAL

A wedge-type, cubic-anvil, high-pressure apparatus was used to prepare ternary metal phosphides at high temperatures and high pressures (8). The upper and lower stages of the apparatus consist of three anvils and slide on the wedge formed in shallow V-shaped grooves. The anvil's movement is completely synchronized by the wedge system. The anvils, prepared from cemented tungsten carbide, have a $16 \times 16\ mm^2$ top-square face. The sample container, made of pyrophyllite, is formed into a cube of 21 mm on the edge. The sample assembly for the preparation of the metal

0022-4596/99 $30.00

phosphides is similar to that used for synthesis of black phosphorus (9). The starting materials are put into a crucible made of BN. The crucible with a graphite heater is inserted into the pyrophyllite cube.

$La_{1-x}Ce_xRu_4P_{12}$ ($x = 0, 0.05, 0.1, 0.2, 0.3, 0.4, 0.5, 0.6, 0.7, 0.75, 0.8, 0.9$, and 1) and $CeOs_4P_{12}$ were prepared by reaction of stoichiometric amounts of each metal and red phosphorus powders at around 1100°C and 4 GPa. The samples were characterized by powder X-ray diffraction using Cu$K\alpha$ radiation and silicon as a standard.

The powder X-ray diffraction patterns of $LaRu_4P_{12}$ and $CeRu_4P_{12}$ were measured with synchrotron radiation monochromatized to 0.6888 Å at atmospheric pressure. An imaging plate was applied to the powder X-ray diffraction experiments (10). Rietveld refinements were carried out with the program Rietan developed by Izumi (11).

Copper or gold leads were attached to the compounds with silver-filled epoxy, and four-lead electrical resistivity measurements were performed at low temperatures. The dc magnetic susceptibility of the compounds was measured in the range 1.8–300 K with a Quantum Design MPMS SQUID magnetometer.

TABLE 1
Positional Parameters and Bond Distances of $CeRu_4P_{12}$

Lattice constant $a = 8.043(1)$ Å
$R_{wp} = 5.54$, $R_{exp} = 1.69$, $S = 3.28$

*Im*3	Ce 2(*a*)	Ru 8(*c*)	P 24(*g*)
x	0.00	0.25	0.0000
y	0.00	0.25	0.3568(5)
z	0.00	0.25	0.1456(4)
U_{11}	0.0090(6)	0.0047(4)	0.003(2)
U_{22}	U_{11}	U_{11}	0.005(3)
U_{33}	U_{11}	U_{11}	0.005(3)
B_{eq}(Å^2)	0.716	0.369	0.389

Bond distances (Å) and bond angles (deg)

Ce–P	3.102(4)	(12×)	P′–P–P″	90.00
–Ru	3.4856	(8×)	Ru–P–R	118.3(1)
Ru–P	2.344(1)	(6×)	Ru–P–P′	111.52(9)
–Ce	3.4856	(2×)	Ru–P–P″	111.02(8)
P–P′	2.305(8)	(1×)	Ce–P–P′	157.81(5)
–P″	2.343(7)	(1×)	Ce–P–P″	67.81(5)
–Ru	2.344(1)	(2×)	Ce–P–Ru	78.2(1)
–P	3.077(4)	(4×)		
–Ce	3.102(4)	(1×)		
–P	3.287(5)	(1×)		

Note: $R_{wp} = 100\{\sum w_i(y_{oi} - y_{ci})^2/\sum w_i(y_{oi})^2\}^{1/2}$; $R_{exp} = 100\{N - P + C)/\sum w_i y_{oi}\}^{1/2}$; $S = R_{wp}/R_{exp}$.

RESULTS AND DISCUSSION

Structure

The crystal structures of $LaRu_4P_{12}$ and $CeRu_4P_{12}$ are refined with the Rietveld method of analyzing powder X-ray diffraction data; the structure is refined by fitting the entire profile of the diffraction pattern to the calculated profile. Figure 1 shows the X-ray diffraction and the calculated profiles of $CeRu_4P_{12}$. The agreement between the observed and calculated patterns is good. The structure of $CeRu_4P_{12}$ is refined to $R_{wp} = 5.54$. The results for $CeRu_4P_{12}$ obtained by the Rietveld analysis are given in Table 1. These results are similar to those for $CeFe_4P_{12}$, which has been determined from single-crystal counter data (12). The skutterudite structure is characterized by formation of rectangular P_4^{4-} clusters. The P–P distances in $CeRu_4P_{12}$ are 2.305 Å along the shorter edge and 2.343 Å along the longer edge.

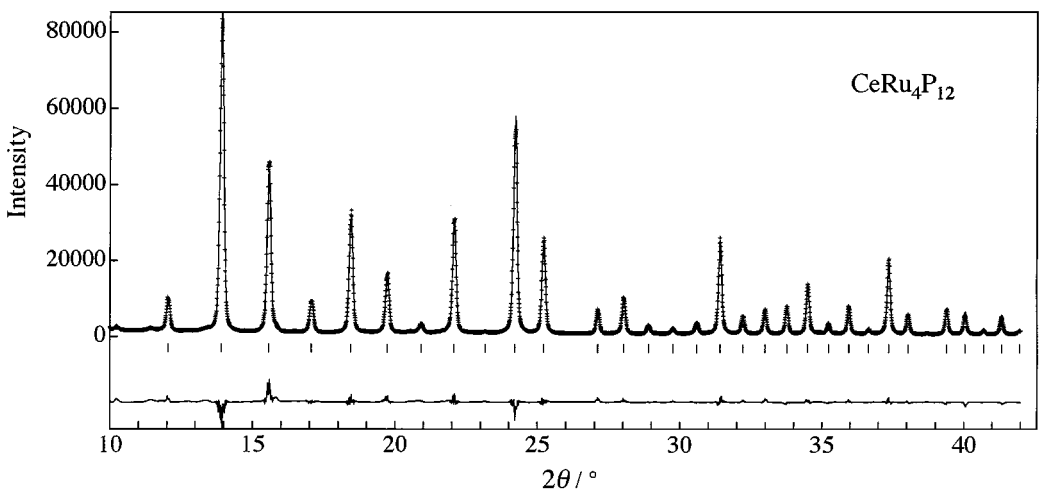

FIG. 1. X-ray diffraction and calculated patterns of $CeRu_4P_{12}$. Plus marks (+) represent the raw data. The solid line is the calculated profile. The vertical marks show the positions of allowed reflections. The differences between the observed and calculated patterns are shown.

TABLE 2
Positional Parameters and Bond Distances of $LaRu_4P_{12}$

Lattice constant $a = 8.061(1)$ Å
$R_{wp} = 4.77$, $R_{exp} = 2.19$, $S = 2.18$

	La	Ru	P
*Im*3	2(*a*)	8(*c*)	24(*g*)
x	0.00	0.25	0.0000
y	0.00	0.25	0.3591(4)
z	0.00	0.25	0.1428(4)
U_{11}	0.0099(5)	0.0070(3)	0.005(2)
U_{22}	U_{11}	U_{11}	0.014(3)
U_{33}	U_{11}	U_{11}	0.008(3)
B_{eq}(Å^2)	0.782	0.556	0.707

Bond distances (Å) and bond angles (deg)

La–P	3.115(4)	(12×)	P′–P–P″	90.00
–Ru	3.4904	(8×)	Ru–P–R	117.10(9)
Ru–P	2.362(1)	(6×)	Ru–P–P′	111.84(8)
–La	3.4904	(2×)	Ru–P–P″	111.45(7)
P–P′	2.272(7)	(1×)	La–P–P′	158.30(4)
–P″	2.303(67)	(1×)	La–P–P″	68.31(4)
–Ru	2.362(1)	(2×)	La–P–Ru	77.84(9)
–P	3.095(3)	(4×)		
–La	3.115(4)	(1×)		
–P	3.235(5)	(1×)		

They are similar to the P–P distances of 2.304 and 2.338 Å in $CeFe_4P_{12}$. The structure of $LaRu_4P_{12}$ has also been refined to $R_{wp} = 4.77$ by Rietveld analysis (Table 2). The Ce–P distance in $CeRu_4P_{12}$ is shorter than the La–P distance in $LaRu_4P_{12}$. The P–P distances in the cerium compound are longer than those in the lanthanum compound.

The compounds CeT_4P_{12} (T = Fe, Ru, and Os) exhibit an anomalously small lattice constant compared to the otherwise smoothly decreasing lattice-parameter variation in going from the La- to the Tb- containing compound. The reduced lattice constants of the Ce compounds suggest the valency +4 for the Ce atoms (1). Figure 2 shows the lattice constant vs concentration (x) curve for $La_{1-x}Ce_xRu_4P_{12}$. The lattice constants of $LaRu_4P_{12}$ and $CeRu_4P_{12}$ obtained by these experiments are 8.061 and 8.043 Å, respectively. The lattice parameters of the alloys do not decrease linearly with increasing x and markedly deviate from linear between $x = 0.4$ and $x = 0.6$. These results suggest that the valency of Ce is +3 for the alloys below $x = 0.6$.

Electrical and Magnetic Properties

The resistivity of $CeRu_4P_{12}$ slowly increases with decreasing temperature from room temperature to 100 K. The activation energy in the temperature region is 0.086 eV. Below 100 K the resistivity rapidly increases with decreasing temperature. Figure 3 shows the temperature

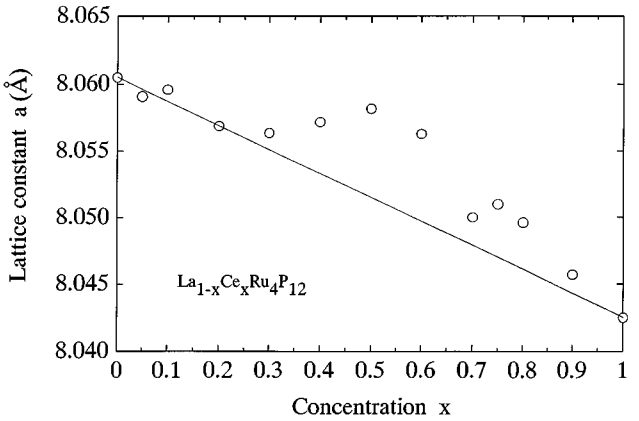

FIG. 2. Lattice constant a vs concentration (x) curve for alloys $La_{1-x}Ce_xRu_4P_{12}$.

dependence of the dc magnetic susceptibility measured in a field of 1 T for $CeRu_4P_{12}$. The susceptibility is insensitive to temperature between 30 and 300 K and rapidly rises at lower temperatures. This upturn at low temperatures arises from a magnetic impurity. The magnetic behavior of $CeRu_4P_{12}$ is very similar to that of $CeFe_4P_{12}$ measured by Meisner *et al.* (3). $CeFe_4P_{12}$ is a semiconductor and shows nearly temperature-independent susceptibility. Meisner *et al.* have suggested that the itinerant *f* electrons present in $CeFe_4P_{12}$ strongly hybridize with the conduction electrons. ESR study of Nd^{3+} and Yb^{3+} in $CeFe_4P_{12}$ supports that there is a strong 4*f*-conduction electron hybridization with an open gap in the density of state at the Fermi level (13). XANES of Ce in $CeFe_4P_{12}$ is complex though the presence of Ce^{3+} is primarily indicated (14). The band calculation suggests that Ce ions are trivalent and Ce 4*f* states in $CeFe_4P_{12}$ hybridize strongly with Fe 3*d* and phosphorus *p* states in the vicinity of the Fermi energy (6).

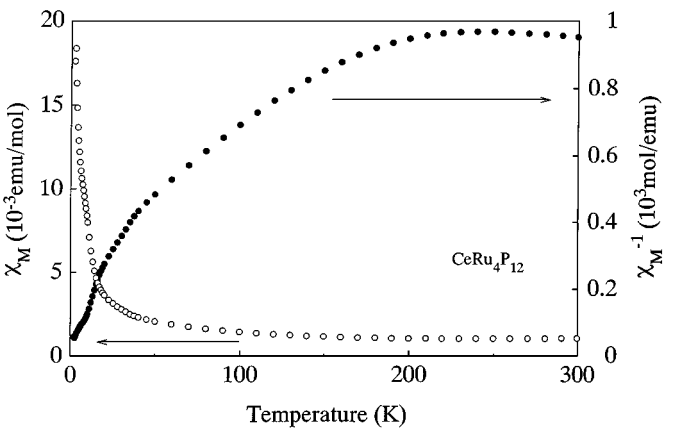

FIG. 3. Magnetic susceptibility vs temperature curves for $CeRu_4P_{12}$.

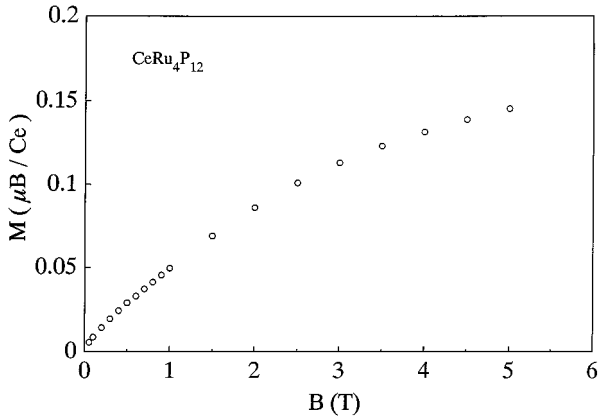

FIG. 4. Magnetization curve of $CeRu_4P_{12}$ at around 2 K.

Figure 4 shows the magnetization curve of $CeRu_4P_{12}$ at around 2 K. This curve at 2 K yields a saturation value of 0.15 μ_B/Ce ion at 5 T. This is much less than the Ce^{3+} free-ion value of 2.54 μ_B/Ce ion. The result suggests that Ce ions in $CeRu_4P_{12}$ are not trivalent, but seem to be close to tetravalent. If Ce in $CeRu_4P_{12}$ is tetravalent, the ionic formula can be described as $Ce^{4+}(Ru_4P_{12})^{4-}$. The Ru atoms in the compound have the d^6 configuration. The susceptibility of $CeRu_4P_{12}$ shows weak paramagnetic behavior resembling that of $CeFe_4P_{12}$. On the other hand, the susceptibility of semiconducting CoP_3 with the d^6 configuration is diamagnetic (15). These results suggest that the valency of Ce in $CeRu_4P_{12}$ is not always +4. The reduced value of magnetization compared to the free-ion value may be due to crystalline electric field effects or hybridization.

Figure 5 shows the electrical resistivity vs temperature curve for $CeOs_4P_{12}$. The resistivity increases with decreasing temperature. This curve can be fit over the temperature range from 120 to 300 K to an activation conduction form, $R = R_0 \exp(\Delta E/k_b T)$, where ΔE is the activation energy and k_b is Boltzmann's constant. The value $\Delta E/k_b$ is about 400 K for $CeOs_4P_{12}$. It has already been reported that the

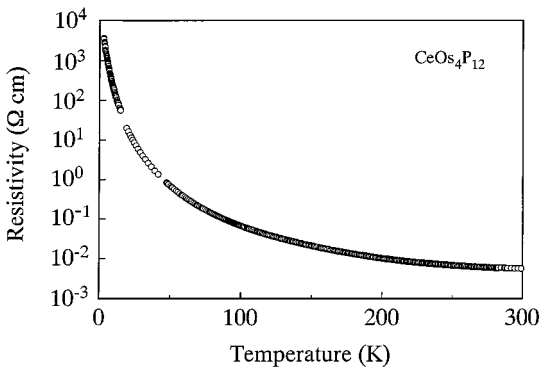

FIG. 5. Electrical resistivity vs temperature curve of $CeOs_4P_{12}$.

TABLE 3
Cell Volumes and Values of $\Delta E/k_b$ in CeT_4P_{12} (T = Fe, Ru, and Os)

Compound	Cell volume (Å^3)	$\Delta E/k_b$ (K)
$CeFe_4P_{12}$	473.1[a]	1500[b]
$CeRu_4P_{12}$	519.3[a]	1000
$CeOs_4P_{12}$	524.1[a]	400

[a] Ref. (1).
[b] Ref. (3).

compounds $CeFe_4P_{12}$ and $CeRu_4P_{12}$ show the semiconducting behavior. The values of $\Delta E/k_b$ and the cell volumes in three Ce compounds are given in Table 3. These values decrease with increasing the cell volume. The energy gap of $CeOs_4P_{12}$ is the lowest in the compounds CeT_4P_{12} (T = Fe, Ru, and Os). The magnetic properties of $CeOs_4P_{12}$ are similar to the results of $CeRu_4P_{12}$ shown in Fig. 3.

The electronic structure of $CeFe_4P_{12}$ has been studied with density-functional calculations (6). The calculation yields a band gap of 0.34 eV at the Fermi energy for $CeFe_4P_{12}$. The valence bands have the character of hybridized Fe 3*d* and phosphorus *p* states. The lowest lying conduction bands are dominated by the narrow spin–orbit split Ce 4*f* band. Ce 4*f* states hybridize strongly with both Fe 3*d* and phosphorus *p* states in the vicinity of the Fermi energy.

The compounds CeT_4P_{12} (T = Fe, Ru, and Os) show similar electrical and magnetic properties. The band structure of $CeRu_4P_{12}$ and $CeOs_4P_{12}$ must resemble that of $CeFe_4P_{12}$. Thus, Ce 4*f* states in CeT_4P_{12} strongly hybridize with T *nd* (n = 3, 4, and 5) and phosphorus *p* states and open the gaps in the vicinity of the Fermi energy. The Ce–P distances in $CeFe_4P_{12}$ and $CeRu_4P_{12}$ are significantly shorter compared with La–P distances in the corresponding lanthanum compounds. The short distance in Ce compounds may be due to the hybridization between Ce 4*f* and phosphorus *p* states.

We have studied the Raman scattering spectra of the compounds $LnRu_4P_{12}$ (Ln = La, Ce, Pr, Nd, Sm, Gd, and Tb) at room temperature (16). The mode at around 440 cm^{-1} is assigned to the vibration involving the Ln atom. The mode near 440 cm^{-1} of the semiconducting $CeRu_4P_{12}$ is very different compared with that of other phosphide-based filled skutterudites behaving as metal. The anomalous behavior of the Ce compound may be closely related to the hybridized electronic state.

Figure 6 shows the resistivity normalized to room temperature of $La_{1-x}Ce_xRu_4P_{12}$ (x = 0.6, 0.7, 0.8, 0.9, and 1.0) at low temperatures. The resistivity of the alloys (x = 0.7, 0.8, and 0.9) and $CeRu_4P_{12}$ increases with decreasing temperature. These materials behave as semiconductors and have activation energies which increase with increasing x.

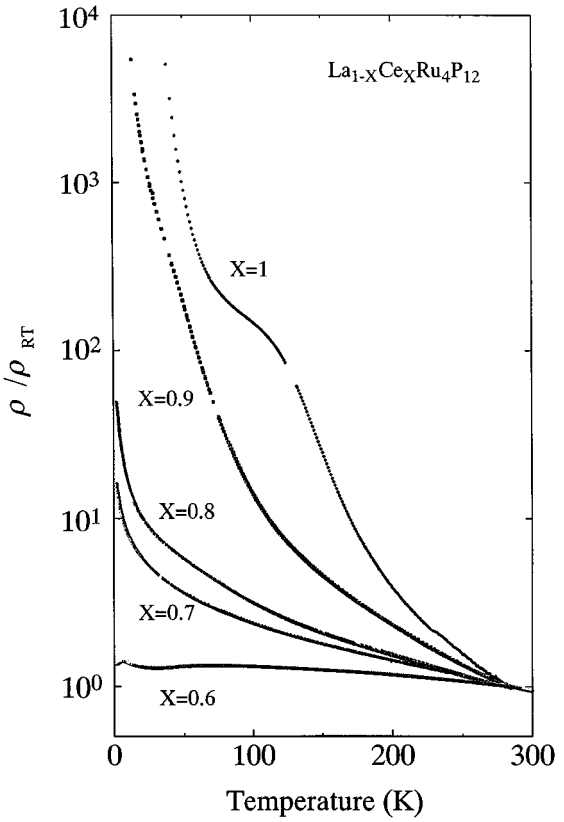

FIG. 6. Resistivity normalized to room temperature of $La_{1-x}Ce_xRu_4P_{12}$ ($x = 0.6$, 0.7, 0.8, 0.9, and 1) at low temperatures.

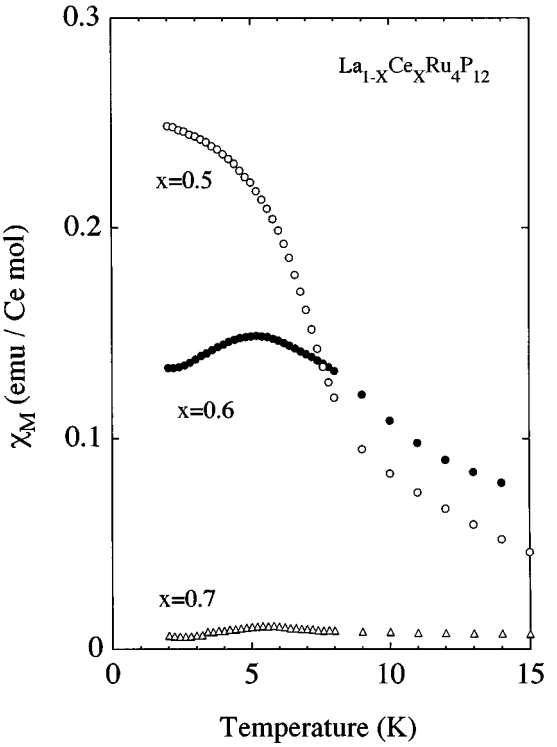

FIG. 7. Magnetic susceptibility vs temperature curves for $La_{1-x}Ce_xRu_4P_{12}$ ($x = 0.5$, 0.6, and 0.7).

On the other hand, the resistivity of $La_{0.4}Ce_{0.6}Ru_4P_{12}$ slightly increases with decreasing temperature. The metal-to-insulator (M–I) transition is observed at around $x = 0.6$. Below $x = 0.5$ the alloys show metallic behavior. The superconducting transition for the alloys ($x = 0$, 0.05, 0.1, and 0.2) is observed between 4 and 7 K (17).

Figure 7 shows the magnetic susceptibilities of $La_{1-x}Ce_xRu_4P_{12}$ ($x = 0.5$, 0.6, and 0.7) at low temperatures. The small maximum in the susceptibility vs temperature curve for $La_{0.4}Ce_{0.6}Ru_4P_{12}$ which shows the M–I transition is observed at around 5 K. The weak magnetic ordering appears between $x = 0.5$ and 0.7. The susceptibility of $La_{0.3}Ce_{0.7}Ru_4P_{12}$ abruptly decreases compared with that of $La_{0.4}Ce_{0.6}Ru_4P_{12}$. The magnetic ordering disappears above $x = 0.75$. The susceptibility vs temperature curves for the alloys ($x = 0.75$, 0.8, and 0.9) are very similar to that of $CeRu_4P_{12}$.

The lattice parameters of $La_{1-x}Ce_xRu_4P_{12}$ deviate from linear between $x = 0.4$ and $x = 0.6$. The valence of the Ce atoms is $+3$ for this region. Thus, there are trivalent Ce ions with one 4*f*-electron in the alloys. The magnetic ordering observed at around $x = 0.6$ arises from *f* electrons in the trivalent Ce ions. Jung *et al.* suggest that the skutterudite compounds are expected to be semiconducting if the transition-metal atoms have the d^6 configuration (5). When Ce in $CeRu_4P_{12}$ is tetravalent, the ruthenium atoms in the compound have the d^6 configuration. If La atoms with a valency of $+3$ are doped into $CeRu_4P_{12}$, the alloys should show metallic behavior as the Ru atoms cannot take the d^6 configuration. However, the alloys with x above 0.7 show semiconducting behavior, being similar to the behavior of $CeRu_4P_{12}$. This result suggests that the Ce 4*f* states in the alloys may also hybridize strongly with Ru 4*d* and phosphorus *p* states in the vicinity of the Fermi energy.

ACKNOWLEDGMENT

The authors thank Tanaka Kikinzoku Kogyo for the gift of the high-purity ruthenium and osmium metal powders.

REFERENCES

1. W. Jeitschko and D. Braun, *Acta Crystallogr., Sect. B* **33,** 3401 (1977).
2. D. J. Braun and W. Jeitschko, *J. Less-Common Met.* **72,** 147 (1980); *J. Solid State Chem.* **32,** 357 (1980).
3. G. P. Meisner, M. S. Torikachvili, K. N. Yang, M. B. Maple, and R. P. Guertin, *J. Appl. Phys*, **57,** 3073 (1985).
4. I. Shirotani, T. Adachi, K. Tachi, S. Todo, K. Nozawa, T. Yagi, and M. Kinoshita, *J. Phys. Chem. Solids* **57,** 211 (1996).

5. D. Jung, M. H. Whangbo, and S. Alvarez, *Inorg. Chem.* **29,** 2252 (1990).
6. L. Nordstrom and D. J. Singh, *Phys. Rev. B* **53,** 1103 (1996).
7. I. Shirotani, *Rev. High Pressure Sci. Technol.* **6,** 109 (1997).
8. I. Shirotani, N. Ichihashi, K. Nozawa, M. Kinoshita, T. Yagi, K. Suzuki, and T. Enoki, *Jpn. J. Appl. Phys., Suppl.* **32,** 695 (1993).
9. I. Shirotani, *Mol. Cryst. Liq. Cryst.* **86,** 1943 (1982).
10. O. Shimomura, K. Takemura, H. Fujihisa, Y. Fujii, Y. Ohishi, T. Kikegawa, Y. Amemiya, and T. Matsushita, *Rev. Sci. Instrum.* **63,** 967 (1992).
11. F. Izumi, *Oyo Buturi* **59,** 2 (1990).
12. F. Grandjean, A. Gerard, D. J. Braun, and W. Jeitschko, *J. Phys. Chem. Solids* **45,** 877 (1984).
13. G. B. Martins, M. A. Pires, G. E. Barberis, C. Rettori, and M. S. Torikachvili, *Phys. Rev. B* **50,** 14822 (1994).
14. J. S. Xue, M. R. Antonio, W. T. White, L. Soderholm, and S. M. Kazularich, *J. Alloys Compd.* **207/208,** 161 (1994).
15. J. Ackermann and A. Wold, *J. Phys. Chem. Solids* **38,** 1013 (1977).
16. C. Sekine, H. Saito, T. Uchiumi, A. Sakai, and I. Shirotani, *Solid State Commun.* **106,** 441 (1998).
17. T. Uchiumi, I. Shirotani, C. Sekine, S. Todo, T. Yagi, Y. Nakazawa, and K. Kanoda, *J. Phys. Chem. Solids*, in press.